Preprints (www.preprints.org) | NOT PEER-REVIEWED | Posted: 10 August 2021 doi:10.20944/preprints202108.0220.v1

Epithelial ablation of Miro1/Rhot1 GTPase leads to mitochondrial dysfunction and lung inflammation by cigarette smoke

Shikha Sharma, Qixin Wang, Thivanka M Muthumalage, and Irfan Rahman*

Department of Environmental Medicine, University of Rochester Medical Center, Rochester, NY, USA

Correspondence should be addressed to:*Irfan Rahman, Ph.D.; Department of Environmental Medicine; University of Rochester Medical Center; Box 850, 601 Elmwood Avenue; Rochester 14642, NY, USA; Tel: 1 585 275 6911; E-mail: irfan_rahman@urmc.rochester.edu

Short running title: Miro1 dependent mitochondrial dysfunction

Abstract: Cigarette smoke (CS) exposure results in lung damage and inflammation through mitochondrial dysfunction. Mitochondria quality control is sustained by Miro1 (Rhot1), a calcium-binding membrane-anchored GTPase by its interaction with PINK1/Parkin during mitophagy. However, the exact mechanism that operates this interaction of mitophagy machinery in Miro1 degradation and CS-induced mitochondrial dysfunction that results in lung inflammation remains unclear. We hypothesized that mitochondrial Miro1 plays an important role in regulating mitophagy machinery and resulting lung inflammation by CS in mouse lung. We showed a role of Miro1 in CS-induced mitochondrial dysfunction and quality control mechanisms. The Rhot1Fl/Fl (WT) and lung epithelial cell-specific Rhot1 KO were exposed to mainstream CS for 3 days (acute) and 4 months (chronic). The cellular infiltration, cytokines, and lung histopathology were studied for the inflammatory response in the lungs. Acute CS exposure showed a notable increase in the total inflammatory cells, macrophages, and neutrophils associated with inflammatory mediators and Miro1 associated mitochondrial quality control proteins Parkin and OPA1. Chronic exposure showed an increase infiltration of total inflammatory cells and neutrophils versus air controls. Histopathological changes, such as pulmonary macrophages and neutrophils were increased in CS exposed mice. The epithelial Miro1 ablation led to augmentation of inflammatory cell infiltration with alteration in the levels of pro-inflammatory cytokines and histopathological changes. Thus, CS induces disruption of mitochondrial quality control mechanisms, and Rhot1/Miro1 mediates the process of CS-induced mitochondrial dysfunction ensuing lung inflammatory responses.

Keywords: MIRO1, mitochondrial dysfunction, cigarette smoke, mitophagy, COPD.

© 2021 by the author(s). Distributed under a Creative Commons CC BY license.

Preprints (www.preprints.org) | NOT PEER-REVIEWED | Posted: 10 August 2021 doi:10.20944/preprints202108.0220.v1

1. Introduction

Cigarette smoke (CS) leads to mitochondrial dysfunction which is associated with lung inflammation (Sundar, Maremanda, & Rahman, 2019). The dysfunction of the mitochondria accelerates the inflammatory process in lung diseases like chronic obstructive pulmonary disease (COPD) (Ahmad et al., 2015). Normal cellular homeostasis and physiology depends on the regulation of mitochondrial function (Ni, Williams, & Ding, 2015). During cellular damages, the dysfunctional mitochondria are generally eliminated by selective degradation – mitophagy (Lazarou et al., 2015). To sustain the quality control of the mitochondria, Miro1 (Rhot1) serves as an essential element in mitochondrial quality control. Rhot1 (Miro1) is a calcium-binding, membrane-anchored GTPase that is required for the calcium-driven movement of the mitochondria on microtubules, especially during mitophagy (Alshaabi et al., 2021; Sundar et al., 2019; Cloonan & Choi, 2016; Lerner et al., 2016). Miro1 also serves a vital role in mitochondrial dynamics by its interaction with Pink1 (PTEN-induced putative kinase 1)/Parkin mitochondrial quality control system by serving as a signal for mitophagy (Bueno et al., 2015; Safiulina et al., 2019). Depolarization of the mitochondrial membrane is responsible for initiating mitophagy in the cells. Following this, the mitochondrial quality control is performed by the stabilization of Pink1 on mitochondrial outer membranes through fission reaction. An E3 ubiquitin ligase, also called as, Parkin is then recruited from the cytosol by the Pink1 for further mitochondrial quality control (Scarffe, Stevens, Dawson, & Dawson, 2014; Sundar et al., 2019). After the recruitment of Parkin, the degradation of a mitochondrial fusion core protein – mitofusin2 (Mfn2) occurs. This allows clearing off of damaged mitochondria from the cell by protein microtubule-associated protein light chain 3 (LC3) in the isolation membranes that further initiates the formation of autophagosome by localization of damaged mitochondria and that in turn fuses with

the lysosomes to remove the dead mitochondrial cells (Ashrafi & Schwarz, 2013; Sekine & Youle, 2018). The Pink1 and Parkin thereby coordinate together during mitophagy to help regulate mitochondrial degradation. The mitochondrial shape and trafficking are maintained by GTPase Miro1 and Miro2. Thus, together they may serve a crucial role in mitochondrial quality control (Nemani et al., 2018). However, the exact mechanism that operates this interaction of PINK1 and MIRO1 and CS-induced mitochondrial dysfunction that results in lung inflammation in COPD, remains unclear.

We hypothesize that the ablation of Miro1 (Rhot1) from lung epithelial cells would result in the dysfunction of mitochondrial quality control (dysfunctional mitophagy). This may in turn exaggerate the adverse effects of cigarette smoke in the lungs, thereby ensuing CS-induced lung inflammation and mitochondrial dysfunction in lung epithelium (Lerner, Sundar, et al., 2016; Sundar et al., 2019). To demonstrate CS-induced disruption in the mitochondrial quality control mechanisms and the role of Rhot1/Miro1 in mediating the process of CS-induced mitochondrial dysfunction, we utilized the epithelial cell-specific partial (heterozygous) and complete (homozygous) Miro1 knockout (Miro1CC10 KO) mouse models which are to exposed to mainstream cigarette smoke. C57/BL6J mice for 3 days (the acute phase), and 4 months (chronic phase). The role of mitochondrial Miro1 and its impact on the progression of lung inflammation along with mitochondrial dysfunction were studied.

2. Materials and Methods

Ethical Approval: Institutional Biosafety

Ethics Statement

The study is approved via the laboratory protocols by the Institutional Biosafety Committee (IBC) of the University of Rochester Medical Center, Rochester, NY, All animal experiments

were approved by the University Committee on Animal Research at the University of Rochester, Protocol no.102204 / 2007-070E, date of approval, January 31, 2019.

2.1. Animal Model and exposure

Rhot1Fl/Fl (WT) and lung epithelial cell-specific Rhot1 KO mice, Rhot1CreCC1 models were exposed to cigarette smoke (CS) for 3 days duration (acute – Rhot1CC10$^{+/-}$ flp Cre and Rhot1CC10$^{+/+}$ flp Cre) and 4 months (chronic – Rhot1CC10$^{+/-}$ flox Cre and Rhot1CC10$^{+/+}$flox Cre) using Baumgartner-Jaeger CSM2082i (cigarette smoke generating machine; CH Technologies, Westwood, NJ, USA) (J. Chen et al., 2019; Sundar et al., 2010; Yang et al., 2021). All the air group mice were exposed to normal air and the same time duration was maintained as for the CS exposure. Hence, the mice groups were divided into two groups – air and CS groups. Animals were 2-4 months old and were housed under standard pathogen-free conditions with a 12/12 h light and dark cycle in the University vivarium facility.

2.2. Cigarette smoke exposure

Cigarette smoke for exposure was generated by using 3R4F (research-grade cigarettes) and the exposure guidelines were followed as per the protocol of the Federal Trade Commission (1 puff/minute of 2 second's time duration with the volume of 35 mL). The mainstream smoke concentration was set at ~250-300 mg/m^3 of TPM value after diluting it with filtered air and the concentration of carbon monoxide (290 to 300 ppm) was monitored in the chamber (Arunachalam, Sundar, Hwang, Yao, & Rahman, 2010; Hwang et al., 2011; Lerner, Lei, Sundar, & Rahman, 2016). A MicroDust Pro-aerosol monitor (Casella CEL, Bedford, UK) was used for CS exposure monitoring and the verification of the readings was performed after the completion of the exposure cycle each day by gravimetric sampling. Simultaneously, all the air group mice

were exposed to the same time duration of normal air as maintained for the CS exposure (Sundar et al., 2010; Yao et al., 2008).

2.3. Collection of bronchoalveolar lavage (BAL)

Mice were injected with 100 mg/kg/bw of pentobarbiturate intraperitoneally and then euthanized. Then cannula was inserted into the trachea of mice and the lungs were lavaged with normal saline (0.6 ml volume; 3 times). The lavage fluid was collected and centrifuged and the separated supernatant samples were stored at -80°C (M. Chen et al., 2017; Rajendrasozhan, Chung, Sundar, Yao, & Rahman, 2010; Wood et al., 2014; Yao et al., 2008).

2.4. Total cell count in BAL fluid

The cell pallet of BAL fluid was resuspended in normal saline (0.9% NaCl; 1ml/vol.) and stained by trypan blue (cell staining dye) and total cell count/ml was determined by cellometer.

2.5. Differential cell count in BAL fluid

For 3 days (acute) exposure, the differential cell count of immune-inflammatory cells (neutrophils, macrophages, CD4, CD8) was done by BD Accuri flow cytometer in BAL fluid. All cells were stained using cell type-specific mAb. Specific cell labeling markers, LY6B.2 Alexa Fluor 488 (conjugated antibody), F4/80 phycoerythrin (conjugated antibody), CD45 allophycocyanin, and CD8a phycoerythrin-Cy5 (conjugated antibodies) for neutrophils, macrophages, leukocytes, and T-lymphocytes were used, respectively.

For four months (chronic) exposure, differential cell counts to check the cell influx in neutrophils and macrophages were performed on cytospin slides with Diff-Quick staining (Cui, Liu, Ip, Liang, & Mak, 2020; Lim, Kim, Lee, Bae, & Kim, 2018). The Diff-Quick staining involves sequential dipping of the slides into different solutions – fixative agent (methanol, blue), solution 1 (eosinophilic, orange), and solution 2 (basophilic, blue) followed by rinsing and

drying. The collected smears are first allowed to dry followed by dipping the slide for one second and repeating it for five times each into a fixative followed by stains 1 and 2. The excess is allowed to drain after each dip. After drying it, the slide is rinsed in distilled water or Weise's buffer (pH 7.2). The tape strip is then stuck to slide (sticky side down) and the excess tape is removed. It is then blotted or allowed to dry in the air for further examination at low power and under oil immersion.

2.6. Inflammatory mediators

Differential levels of inflammatory mediators in BAL fluid were assessed for their alteration in the levels using Bio-Plex Pro Mouse Cytokine 23-Plex Immunoassay was run using Luminex. Experiments were done following the manufacturer's instructions and the results were presented as pg/mg protein in the samples.

2.7. Measurement of lung mechanics

The mechanical parameters of the lungs like lung resistance, tissue elastance, and static compliance were measured by Flex-ivent apparatus (Scireq; Montreal, Canada). All the mice were weighed and anesthetized by pentobarbital (90 mg/kg; *i.p.* injection) followed by pancuronium (0.5 mg/kg; *i.p.* injection). Mice were then tracheostomized and cannulated and the cannula was attached to the rodent ventilator and the ventilator was connected to a computer (Hwang et al., 2011; Phillips et al., 2015). Measurements of all lung mechanical parameters were repeated three times for all mice.

2.8. Lung Morphometry and histopathology

Mouse lungs were isolated and inflated with 1% agarose (low melting) and fixed with 4% neutral-buffered paraformaldehyde (Yao et al., 2010). Dehydration of the fixed tissue was done followed by encasing it in paraffin and sections were cut by rotary microtome. The lung

midsagittal section of each tissue was stained with H&E (hematoxylin and eosin) and the Lm (linear intercept) of airspace and pathological changes were determined in lung tissues.

2.9. Statistical Analysis

Statistical analysis was done by one-way (ANOVA), Tuckey's post-hock multiple group comparison test by GraphPad Prism 9 software. Data were shown as mean ± SEM. Significance compared between corresponding Air and CS groups of same genotypes as well as in different genotypes. $P < 0.05$ is considered significant.

3. Results

CS-induced inflammatory cell infiltration and differential expression of cytokines were observed in lung epithelial cell-specific Rhot1 deleted mice after 3 days and 4 months of CS exposure.

3.1. Three days (acute) exposure

3.1.1. Inflammatory cellular influx in Rhot1 epithelial cell specific KO (Rhot1 $^{+/-}$CreCC10 and Rhot1$^{-/-}$CreCC10) and WT (Rhot1 Flp) mice

The total number of cells and macrophage count increased significantly in WT (Rhot1 Flp), Rhot1 epithelial cell specific KO (Rhot1 $^{+/-}$CreCC10 and Rhot1$^{-/-}$CreCC10) mice exposed to CS for 3 days. However, none of the groups showed significant changes in the levels of neutrophils, CD4 and CD8 in response to CS exposure (Figure 1).

3.1.2. Effect of acute, CS exposure on levels of pro-inflammatory mediators in Rhot1 epithelial cell specific KO (Rhot1 $^{+/-}$CreCC10 and Rhot1$^{-/-}$CreCC10) and WT (Rhot1 Flp) mice

3.1.3. WT (Rhot1 Flp) mice exposed to 3 days CS showed increasing trends of several pro-inflammatory mediators but the changes between the air and CS group were not found significant. CS exposed Rhot1 epithelial cell specific KO (Rhot1 $^{+/-}$CreCC10 and Rhot1$^{-/-}$

CreCC10) mice showed significant reduction in the levels of MCP1, IL5, Il-1a, IL-3, IL-9, IFN-γ and TNF-α. The rest of the mediators were not significantly affected (Figure 2).

3.1.4. Four Months (chronic) exposure

3.1.5. Inflammatory cellular influx in Rhot1 epithelial cell specific KO (Rhot1 $^{+/-}$CreCC10 and Rhot1$^{-/-}$CreCC10) and WT (Rhot1 Flox) mice

CS exposure significantly increased the total cells and neutrophils (%) in WT (Rhot1$^{fl/fl}$) and Rhot1^{CreCC10} (Rhot1CC10$^{-/-}$Flox Cre and Rhot1CC10$^{+/-}$flox cre) mice. Non-significant, but increasing trends observed in macrophage (%) in CS exposed groups (Figure 3).

3.1.6. Effect of acute, CS exposure on levels of pro-inflammatory mediators in Rhot1 epithelial cell specific KO (Rhot1 $^{+/-}$CreCC10 and Rhot1$^{-/-}$CreCC10) and WT (Rhot1 Flox) mice.

WT (Rhot1 Flox) mice exposed to chronic 4 months CS showed a significant increase and non-significant increasing trends of several pro-inflammatory mediators. CS exposed WT (Rhot1 Flox) and Rhot1 epithelial cell specific KO (Rhot1 $^{+/-}$CreCC10 and Rhot1$^{-/-}$CreCC10) mice showed significant increase in the levels of MCP1, KC, TNF-α, IL12p40, MIP1-a ,IL-17p70. However, IL-13, IL-10, MIP1-β showed a significant increase only in Rhot1 epithelial cell specific KO (Rhot1 $^{+/-}$CreCC10 and Rhot1$^{-/-}$CreCC10) .The rest of the mediators were not affected significantly (Figure 4).

3.1.7. Effect of CS on lung mechanical properties in Rhot1 epithelial cell specific KO (Rhot1 $^{+/-}$CreCC10 and Rhot1$^{-/-}$CreCC10) and WT (Rhot1 Flox) mice

3.1.8. WT Rhot1 Flox mice exposed to CS showed non-significant increasing trends in resistance and compliance and a decreasing trend in elastance, In contrast, KO (Rhot1 $^{+/-}$CreCC10 and Rhot1$^{-/-}$CreCC10) mice exposed to CS did not show any observable changes in

resistance, elastance and compliance (Figure 4). Airspace enlargement also did not show much appreciable changes though there was a trend in CS exposed mouse lungs (Figure 5).

3.1.9. Effect on airspace enlargement and pathology of lung tissues in Rhot1 epithelial cell specific KO (Rhot1 $^{+/-}$CreCC10 and Rhot1$^{-/-}$CreCC10) and WT (Rhot1 Floxed) mice

Lung sections from chronic 4 months CS-exposed Rhot1 CC10$^{+/-}$ Floxed Cre mice did not show significant airspace enlargement in comparison with air and CS-exposed Rhot1$^{fl/fl}$ (WT) mice. However, other histopathological changes such as interstitial foamy macrophages and neutrophils are found in CS exposed mice and the changes are more intensified in Rhot1 CC10$^{+/-}$ Flox Cre mice (Figure 6).

4. Discussion

Chronic inflammation of the lungs is the hallmark in the pathogenesis of COPD, which is primarily caused by cigarette smoking. The smoke of cigarettes contains large amounts of toxic chemicals that affect the cells of the lungs by deleterious nature of tobacco smoke (Nyunoya et al., 2014; Yao et al., 2012). The dysfunction in mitochondria due to injury and morphological alterations are shown to be significantly driven by the CS exposure to the lung cells that includes airway and alveolar epithelial cells, fibroblasts, and airway smooth muscle cells (Aravamudan et al., 2014; Ballweg, Mutze, Konigshoff, Eickelberg, & Meiners, 2014; Hara et al., 2013). However, the mechanism behind this cellular damage and inflammatory response, and the role of Miro1 in mitochondrial dysfunction upon exposure to CS in lung epithelial cells has remained unclear. In this study, the Rhot1Fl/Fl (WT) and lung epithelial cell-specific Rhot1 KO mice were exposed to CS on acute (3 days) and chronic duration (4 months) to examine the role of Rhot1/Miro1 in the CS-disrupted mitochondrial quality control mechanisms and inflammatory response. The role of mitochondrial dysregulation in lung inflammatory diseases like COPD is

known (Mizumura et al., 2014; Wiegman et al., 2015). Regulation of cellular events like fission (fragmentation) and fusion (elongation) process allows mitochondria to rapidly change their shape. MFNs (membrane-anchored proteins: Mfn1 and 2) and OPA-1 (optic atrophy 1) are the major proteins that allow mitochondrial fusion by interacting with other proteins like Pink1 in the mitochondrial membranes (Y. Chen & Dorn, 2013). We analyzed the differential abundance of mitochondrial fission and fusion proteins in lung epithelial cell-specific Rhot1 KO mice through immunoblot analysis. It was found that the levels of OPA1 (a fusion protein) and parkin (which identifies the damaged mitochondria for mitophagy) were significantly reduced with CS exposure (data not shown). This further demonstrate the role of different mitochondrial proteins in mitochondrial functioning and how it alters the mitochondrial quality control mechanism. The mitochondrial control protein, like Miro1 is targeted by Pink1 and Parkin for mitophagy in the damaged mitochondria. Hence reduction in these proteins may explain the impaired mitophagy response to CS (Birsa et al., 2014); (Kazlauskaite et al., 2014); Wang et al., 2011). The mitochondrial dysregulation was also evident in our study by the increase in the lung infiltraton of total inflammatory cells, macrophages, and neutrophils in the mice models after acute and chronic exposure of CS that were analyzed from the bronchoalveolar lavage (BAL) fluid in the mice. However, there was no change noted in the CD4 and CD8 counts. Inflammatory mediators/biomarkers, like MCP1, IL5, Il-1a, IL-3, IL-9, IFN-γ, and TNF-α were significantly affected after acute CS exposure. In contrast, MCP1, KC, TNF-α, IL12p40, MIP1-a, IL-17p70 both in WT and Miro1 epithelial cellular KO groups along with IL-13, IL-10 and MIP1-β were significantly abundant only in Miro1 epithelial cellular KO groups after chronic exposure. Further, other cytokines did not show significant trends for any changes. Further, other cytokines did not show significant trends for any changes. It is known that any accumulation of infiltrating

cells like neutrophils and macrophages increases along with inflammatory cells are the prime events in the pathological contribution of smoking to lung (Domínguez-Fandos et al., 2012; Gorska et al., 2008). The disruptions in the mitochondria refer to various events that occur at the cellular level in the mitochondria, such as morphological changes, alteration in its metabolic activity, decreased membrane potential and altered mitochondrial superoxide levels and intracellular Ca2+ flux (Cloonan & Choi, 2016; Lerner, Sundar, et al., 2016). This may alter the dynamic nature of the organelle. CS exposure causes an alteration in this dysregulation of mitochondria by modifying its function, mitophagy and resulting in ROS production (Ahmad et al., 2015; Hara et al., 2013). The histopathological data of the lung sections after 4 months of CS-exposure in Rhot1 CC10$^{+/-}$ Flox Cre mice did not reveal any significant airspace enlargement in comparison with air and CS-exposed Rhot1fl/fl (WT) mice. Nevertheless, other changes, such as accumulation of pulmonary macrophages and signs of epithelial hyperplasia dysplasia at airway region of the CS exposed mouse lungs were observed. The changes are more intensified in Rhot1 CC10+/- Flox Cre mice. The inflammation of the lungs impacts the airways with smaller airways being more predominant at the early stages (Domínguez-Fandos et al., 2012; Lerner, Sundar, et al., 2016). Mechanical properties and airspace enlargement of lungs had no comparable changes of Rhot1 to air and CS groups as well as to WT and KO groups. Shorter duration and amount of cigarette smoke may explain the non-significance of structural changes. However, the reduced levels of quality proteins indicate that our results are in consistent with previous studies that have shown reduced proteins along with the increase in the levels of ROS in the damaged mitochondria in the lung epithelial cells when exposed to CS (Ito et al., 2015; Kobayashi et al., 2016; Sundar et al., 2019). The explanation for this disutpion of mitochondrial quality control proteins including Pink1/Parkin may be regulated by Miro1 (Kazlauskaite et al.,

2014). The increased expression of mitochondrial quality control proteins and their role in mitochondrial dysfunction was not assessed which again contributed to the limitation of the study. Additional studies have also shown that the overexpression of quality control proteins like Parkin may restore mitophagy in CS exposed cells by decreasing the cellular senescence (Ahmad et al., 2015; Ballweg et al., 2014; Hara et al., 2013). There are several studies that point PINK1/Parkin-dependent mitophagy and the role of Miro1 (Rhot1) and Miro2 (Rhot2) in it (Klosowiak et al., 2016; Kondapalli et al., 2012; Lopez-Domenech et al., 2018; Safiulina et al., 2019) . This may yield insights into the strategies that focus to pharmacologically restore the role of mitochondrial quality control proteins to treat lung inflammatory conditions like COPD.

Conclusion

Epithelial Miro1 ablation was shown to augment the inflammatory cell infiltration with alteration in the levels of pro-inflammatory cytokines and histopathological changes in mouse lungs (Figure 7). The study thereby establishes the hypothesis that CS induces disruption in mitochondrial quality control mechanisms, and Rhot1/Miro1 is the key regulator of mitochondrial motility during mitophagy that mediates the process of CS-induced mitochondrial dysfunction.

Acknowledgments: The National Institutes of Health (NIH) 1R01HL135613, R01 ES029177, HL137738, and R01 HL133404 supported this study. The funding body has no role in design of the study, data collection, analysis, and interpretation of data and in writing the manuscript. We thank Dr. Isaac Sundar for providing scientific/technical inputs. Dr. Krishna Maremanda provided acute exposure and cell counts as a part of technical assistance, and Dr. Lakshmi

Chakrapani for technical assistance. We also thank our technical staff Daria M Krenitsky for helping us with tissue sectioning and H&E staining.

Authors Contributions: SS designed and conducted the experiments; IR conceived the concept and ideas; TM Performed exposure design, mouse experiments, flow data analysis, and scientific input; QW Performed mouse sacrifice and exposures, histology, Lm, and data analysis; TM edited the manuscript, SS and IR wrote and/or edited/revised the manuscript. IR obtained research funding.

Declarations and Disclosures: Conflict of or competing interest statement

The authors have declared that no competing interests exist.

References

Ahmad, T., Sundar, I. K., Lerner, C. A., Gerloff, J., Tormos, A. M., Yao, H., & Rahman, I. (2015). Impaired mitophagy leads to cigarette smoke stress induced cellular senescence: implications for chronic obstructive pulmonary disease. The FASEB Journal, 29(7), 2912–2929.

Alshaabi, H., Shannon, N., Gravelle, R., Milczarek, S., Messier, T., & Cunniff, B. (2021). Miro1-mediated mitochondrial positioning supports subcellular redox status. Redox Biology, 38, 101818.

Aravamudan, B., Kiel, A., Freeman, M., Delmotte, P., Thompson, M., Vassallo, R., . Prakash, Y. S. (2014). Cigarette smoke-induced mitochondrial fragmentation and dysfunction in human airway smooth muscle. American Journal of Physiology-Lung Cellular and Molecular Physiology, 306(9), L840–L854.

Arunachalam, G., Sundar, I. K., Hwang, J., Yao, H., & Rahman, I. (2010). Emphysema is associated with increased inflammation in lungs of atherosclerosis-prone mice by cigarette smoke: implications in comorbidities of COPD. Journal of Inflammation, 7(1), 1–10.

Ashrafi, G., & Schwarz, T. L. (2013). The pathways of mitophagy for quality control and clearance of mitochondria. Cell Death & Differentiation,

Ballweg, K., Mutze, K., Konigshoff, M., Eickelberg, O., & Meiners, S. (2014). Cigarette smoke extract affects mitochondrial function in alveolar epithelial cells. American Journal of Physiology-Lung Cellular and Molecular Physiology, 307(11), L895–L907.

Birsa, N., Norkett, R., Wauer, T., Mevissen, T. E. T., Wu, H.-C., Foltynie, T., . Plun-Favreau, H. (2014). Lysine 27 ubiquitination of the mitochondrial transport protein Miro is dependent on serine 65 of the Parkin ubiquitin ligase. Journal of Biological Chemistry, 289(21), 14569–14582.

Bueno, M., Lai, Y.-C., Romero, Y., Brands, J., Croix, C. M. S., Kamga, C., . Lee, J. S. (2015). PINK1 deficiency impairs mitochondrial homeostasis and promotes lung fibrosis. The Journal of Clinical Investigation, 125(2), 521–538.

Chen, J., Dai, L., Wang, T., He, J., Wang, Y., & Wen, F. (2019). The elevated CXCL5 levels in circulation are associated with lung function decline in COPD patients and cigarette smoking-induced mouse model of COPD. Annals of Medicine, 51(5–6), 314–329.

Chen, M., Wang, T., Shen, Y., Xu, D., Li, X., An, J., . Chen, L. (2017). Knockout of RAGE ameliorates mainstream cigarette smoke-induced airway inflammation in mice. International Immunopharmacology, 50, 230–235.

Chen, Y., & Dorn, G. W. (2013). PINK1-phosphorylated mitofusin 2 is a Parkin receptor for culling damaged mitochondria. Science, 340(6131), 471–475.

Cloonan, S. M., & Choi, A. M. K. (2016). Mitochondria in lung disease. The Journal of Clinical Investigation, 126(3), 809–820.

Cui, Y., Liu, K. W. K., Ip, M. S. M., Liang, Y., & Mak, J. C. W. (2020). Protective effect of selegiline on cigarette smoke-induced oxidative stress and inflammation in rat lungs in vivo. Annals of Translational Medicine, 8(21).

Domínguez-Fandos, D., Peinado, V. I., Puig-Pey, R., Ferrer, E., Musri, M. M., Ramírez, J., & Barberà, J. A. (2012). Pulmonary Inflammatory Reaction and Structural Changes Induced by Cigarette Smoke Exposure in the Guinea Pig. COPD: Journal of Chronic Obstructive Pulmonary Disease, 9(5), 473–484.

Gorska, K., Krenke, R., Korczynski, P., Kosciuch, J., Domagala-Kulawik, J., & Chazan, R. (2008). Eosinophilic airway inflammation in chronic obstructive pulmonary disease and asthma. J Physiol Pharmacol, 59(Suppl 6), 261–270.

Hara, H., Araya, J., Ito, S., Kobayashi, K., Takasaka, N., Yoshii, Y., . Numata, T. (2013). Mitochondrial fragmentation in cigarette smoke-induced bronchial epithelial cell senescence. American Journal of Physiology-Lung Cellular and Molecular Physiology, 305(10), L737–L746.

Hwang, J., Rajendrasozhan, S., Yao, H., Chung, S., Sundar, I. K., Huyck, H. L., . Rahman, I. (2011). FOXO3 deficiency leads to increased susceptibility to cigarette smoke-induced inflammation, airspace enlargement, and chronic obstructive pulmonary disease. The Journal of Immunology, 187(2), 987–998.

Ito, S., Araya, J., Kurita, Y., Kobayashi, K., Takasaka, N., Yoshida, M., . Fujii, S. (2015). PARK2-mediated mitophagy is involved in regulation of HBEC senescence in COPD pathogenesis. Autophagy, 11(3), 547–559.

Kazlauskaite, A., Kelly, V., Johnson, C., Baillie, C., Hastie, C. J., Peggie, M., . Pedrioli, P. G. A. (2014). Phosphorylation of Parkin at Serine65 is essential for activation: elaboration of a Miro1 substrate-based assay of Parkin E3 ligase activity.

Klosowiak, J. L., Park, S., Smith, K. P., French, M. E., Focia, P. J., Freymann, D. M., & Rice, S. E. (2016). Structural insights into Parkin substrate lysine targeting from minimal Miro substrates. Scientific Reports, 6(1), 1–13.

Kobayashi, K., Araya, J., Minagawa, S., Hara, H., Saito, N., Kadota, T., . Kurita, Y. (2016). Involvement of PARK2-mediated mitophagy in idiopathic pulmonary fibrosis pathogenesis. The Journal of Immunology, 197(2), 504–516.

Kondapalli, C., Kazlauskaite, A., Zhang, N., Woodroof, H. I., Campbell, D. G., Gourlay, R., . Deak, M. (2012). PINK1 is activated by mitochondrial membrane potential depolarization and stimulates Parkin E3 ligase activity by phosphorylating Serine 65. Open Biology, 2(5), 120080.

Lazarou, M., Sliter, D. A., Kane, L. A., Sarraf, S. A., Wang, C., Burman, J. L., . Youle, R. J. (2015). The ubiquitin kinase PINK1 recruits autophagy receptors to induce mitophagy. Nature, 524(7565), 309–314.

Lerner, C. A., Lei, W., Sundar, I. K., & Rahman, I. (2016). Genetic ablation of CXCR2 protects against cigarette smoke-induced lung inflammation and injury. Frontiers in Pharmacology, 7, 391.

Lerner, C. A., Sundar, I. K., & Rahman, I. (2016). Mitochondrial redox system, dynamics, and dysfunction in lung inflammaging and COPD. The International Journal of Biochemistry & Cell Biology, 81, 294–306.

Lim, D., Kim, W., Lee, C., Bae, H., & Kim, J. (2018). Macrophage depletion protects against cigarette smoke-induced inflammatory response in the mouse colon and lung. Frontiers in Physiology, 9, 47.

Lopez-Domenech, G., Covill-Cooke, C., Howden, J. H., Birsa, N., Morfill, C., Brandon, N. J., & Kittler, J. T. (2018). Miro ubiquitination is critical for efficient damage-induced PINK1/Parkin-mediated mitophagy. BioRxiv,

Mizumura, K., Cloonan, S. M., Nakahira, K., Bhashyam, A. R., Cervo, M., Kitada, T., . Washko, G. R. (2014). Mitophagy-dependent necroptosis contributes to the pathogenesis of COPD. The Journal of Clinical Investigation, 124(9), 3987–4003.

Nemani, N., Carvalho, E., Tomar, D., Dong, Z., Ketschek, A., Breves, S. L., . Palaniappan, P. (2018). MIRO-1 determines mitochondrial shape transition upon GPCR activation and Ca2+ stress. Cell Reports, 23(4), 1005–1019.

Ni, H.-M., Williams, J. A., & Ding, W.-X. (2015). Mitochondrial dynamics and mitochondrial quality control. Redox Biology, 4, 6–13.

Nyunoya, T., Mebratu, Y., Contreras, A., Delgado, M., Chand, H. S., & Tesfaigzi, Y. (2014). Molecular processes that drive cigarette smoke-induced epithelial cell fate of the lung. American Journal of Respiratory Cell and Molecular Biology, 50(3), 471–482.

Phillips, B., Veljkovic, E., Peck, M. J., Buettner, A., Elamin, A., Guedj, E., . Bou, S. (2015). A 7-month cigarette smoke inhalation study in C57BL/6 mice demonstrates reduced lung

inflammation and emphysema following smoking cessation or aerosol exposure from a prototypic modified risk tobacco product. Food and Chemical Toxicology, 80, 328–345.

Rajendrasozhan, S., Chung, S., Sundar, I. K., Yao, H., & Rahman, I. (2010). Targeted disruption of NF- B1 (p50) augments cigarette smoke-induced lung inflammation and emphysema in mice: a critical role of p50 in chromatin remodeling. American Journal of Physiology-Lung Cellular and Molecular Physiology, 298(2),

Safiulina, D., Kuum, M., Choubey, V., Gogichaishvili, N., Liiv, J., Hickey, M. A., . Liiv, M. (2019). Miro proteins prime mitochondria for Parkin translocation and mitophagy. The EMBO Journal, 38(2), e99384.

Scarffe, L. A., Stevens, D. A., Dawson, V. L., & Dawson, T. M. (2014). Parkin and PINK1: much more than mitophagy. Trends in Neurosciences, 37(6), 315–324.

Sekine, S., & Youle, R. J. (2018). PINK1 import regulation; a fine system to convey mitochondrial stress to the cytosol. BMC Biology, 16(1), 1–12.

Sundar, I. K., Chung, S., Hwang, J.-W., Arunachalam, G., Cook, S., Yao, H., . Rahman, I. (2010). Peroxiredoxin 6 differentially regulates acute and chronic cigarette smoke mediated lung inflammatory response and injury. Experimental Lung Research, 36(8), 451–462.

Sundar, I. K., Maremanda, K. P., & Rahman, I. (2019). Mitochondrial dysfunction is associated with Miro1 reduction in lung epithelial cells by cigarette smoke. Toxicology Letters, 317, 92–101.

Wiegman, C. H., Michaeloudes, C., Haji, G., Narang, P., Clarke, C. J., Russell, K. E., . Kanerva, J. (2015). Oxidative stress-induced mitochondrial dysfunction drives inflammation and

airway smooth muscle remodeling in patients with chronic obstructive pulmonary disease. Journal of Allergy and Clinical Immunology, 136(3), 769–780.

Wood, T. T., Winden, D. R., Marlor, D. R., Wright, A. J., Jones, C. M., Chavarria, M., . Reynolds, P. R. (2014). Acute secondhand smoke-induced pulmonary inflammation is diminished in RAGE knockout mice. American Journal of Physiology-Lung Cellular and Molecular Physiology, 307(10), L758–L764.

Yang, D., Xu, D., Wang, T., Yuan, Z., Liu, L., Shen, Y., & Wen, F. (2021). Mitoquinone ameliorates cigarette smoke-induced airway inflammation and mucus hypersecretion in mice. International Immunopharmacology, 90, 107149.

Yao, H., Chung, S., Hwang, J., Rajendrasozhan, S., Sundar, I. K., Dean, D. A., . Rnty, M. (2012). SIRT1 protects against emphysema via FOXO3-mediated reduction of premature senescence in mice. The Journal of Clinical Investigation, 122(6), 2032–2045.

Yao, H., Edirisinghe, I., Rajendrasozhan, S., Yang, S.-R., Caito, S., Adenuga, D., & Rahman, I. (2008). Cigarette smoke-mediated inflammatory and oxidative responses are strain-dependent in mice. American Journal of Physiology-Lung Cellular and Molecular Physiology, 294(6),L1174–L1186. Retrieved from https://journals.physiology.org/doi/abs/10.1152/ajplung.00439.2007

Figure and Figure Legends

Figure 1

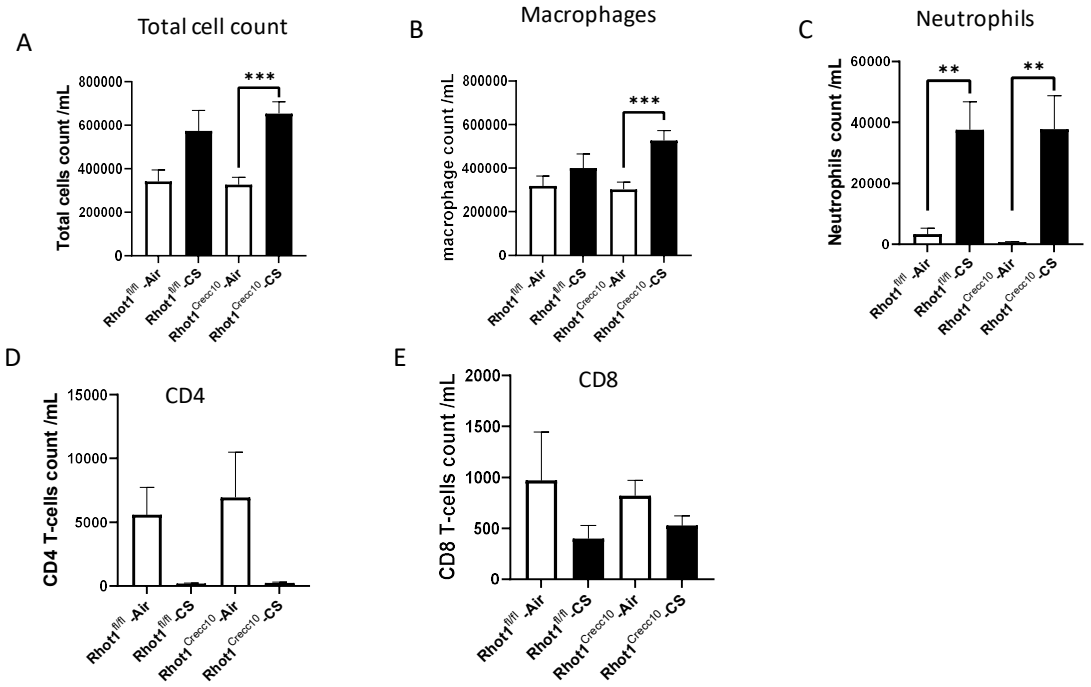

Figure 1: CS induced cell infiltration in lung epithelial cell–specific Rhot1 deleted mice: Rhot1$^{Fl/Fl}$ (WT) and Rhot1^{CreCC10} (Rhot1 flp CreCC10$^{+/-}$ and Rhot1 flp CreCC10$^{+/+}$) mice were exposed to room air and CS (mainstream) for 3 days (acute exposure).

Differential cell count in BAL fluid rom air and CS-exposed mice for 3 days was determined. Alteration in **A.** Total cell count **B.** Macrophages **C**. Neutrophils **D.** CD4 and **E**. CD8, occurred due to CS exposure. Significance compared between corresponding Air and CS groups and all the groups compared with each other irrespective of their exposures. Data are shown as mean ± SEM (n=5 to 13 per group). $^{**}P < 0.01$, $^{***}P < 0.0001$

Figure 2

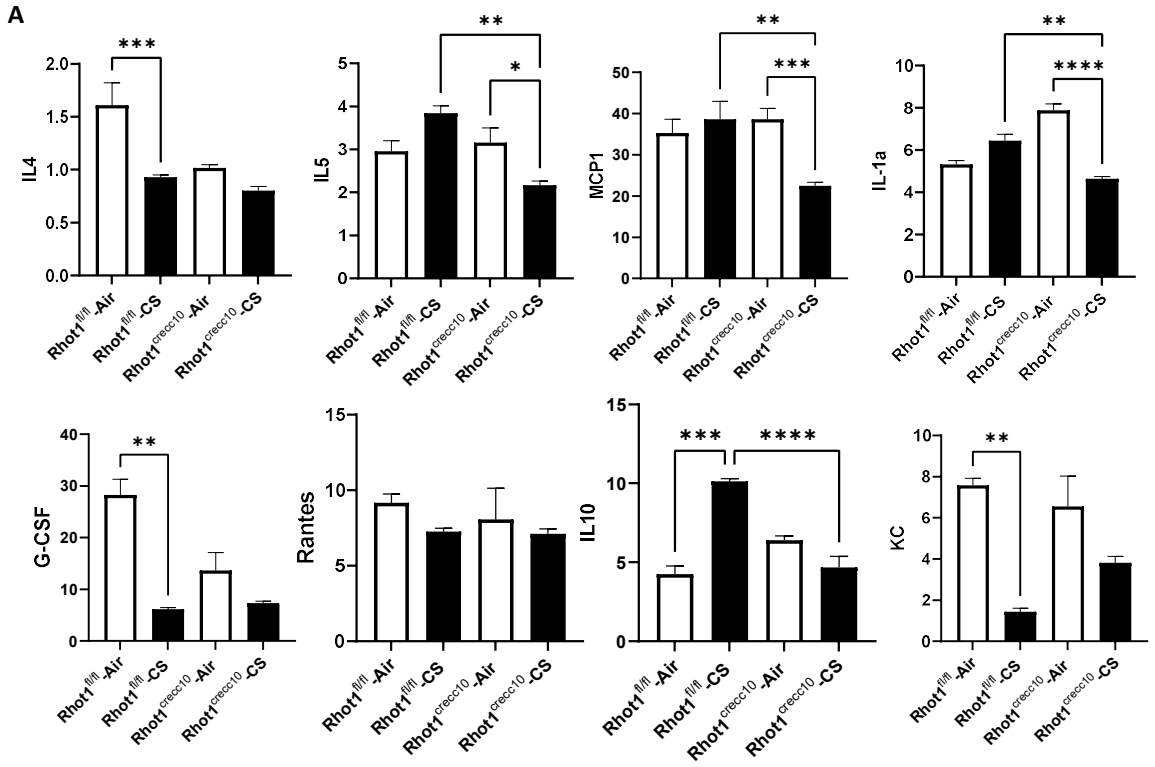
A
IL4
IL5
MCP1
IL-1a
G-CSF
Rantes
IL10
KC
Rhot1 fl/fl -Air
Rhot1 fl/fl -CS
Rhot1 crecc10 -Air
Rhot1 crecc10 -CS

Figure 2

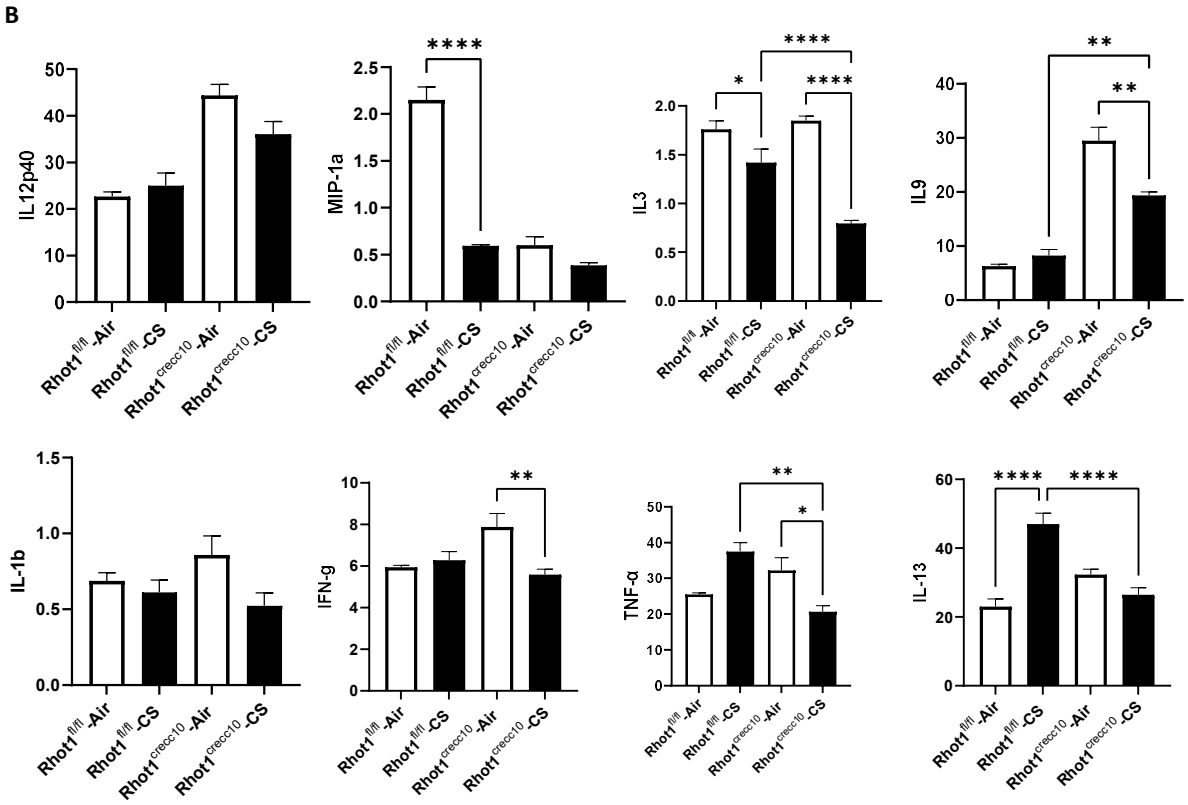
B
IL12p40
MIP-1a
IL3
IL9
IL-1b
IFN-g
TNF-α
IL-13
Rhot1 fl/fl -Air
Rhot1 fl/fl -CS
Rhot1 crecc10 -Air
Rhot1 crecc10 -CS
****
*
**

Figure 2

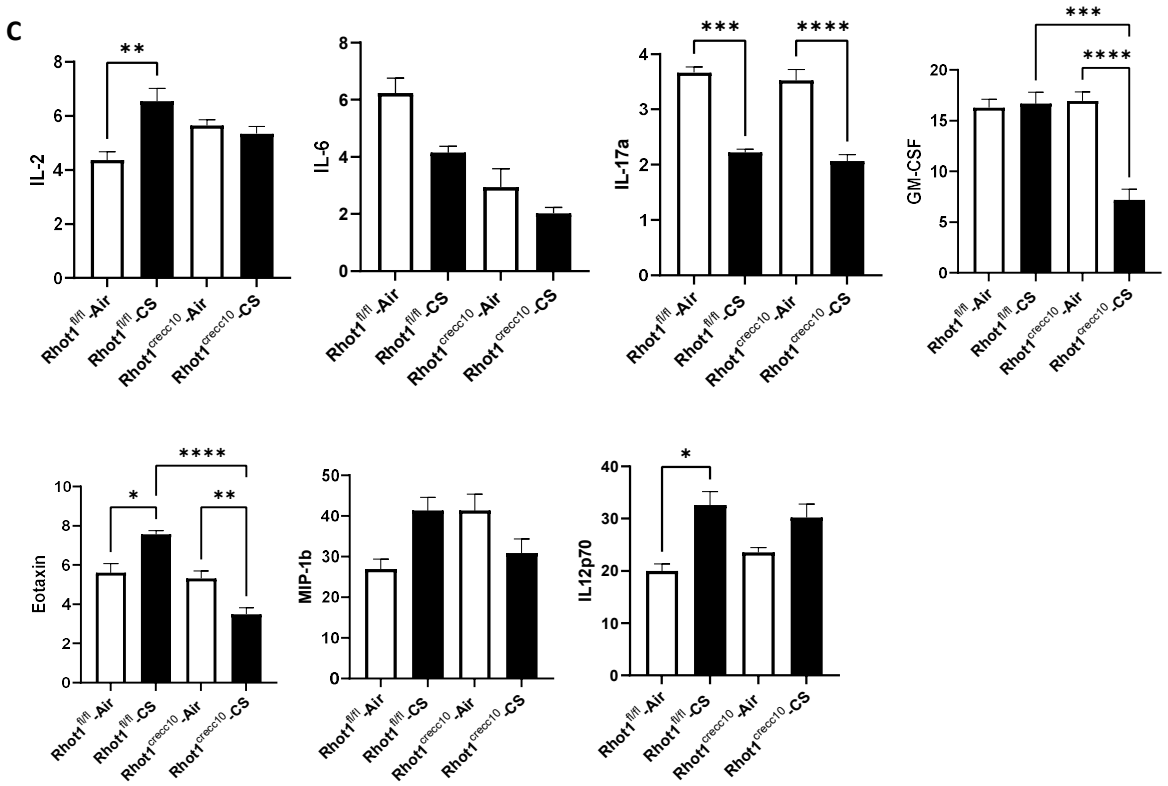

Figure 2: Differential expression of cytokines in epithelial cell–specific Rhot1 deleted and WT mice. A-C: Rhot1$^{Fl/Fl}$ (WT) and Rhot1^{CreCC10} (Rhot1 flp CreCC10$^{+/-}$ and Rhot1 flp CreCC10$^{+/+}$) mice were exposed to room air and CS (mainstream) for 3 days (acute exposure). Expression levels of pro-inflammatory and inflammatory mediators in BAL fluid rom air and CS-exposed mice for 3 days was determined using Bio-Plex Pro 23-plex cytokine assay. Significance compared between corresponding Air and CS groups and all the groups compared with each other irrespective of their exposures. Data are shown as mean ± SEM (n=5 to 13 per group). *$P < 0.05$, **$P < 0.01$, ***$P < 0.001$, ****$P < 0.0001$

Figure 3

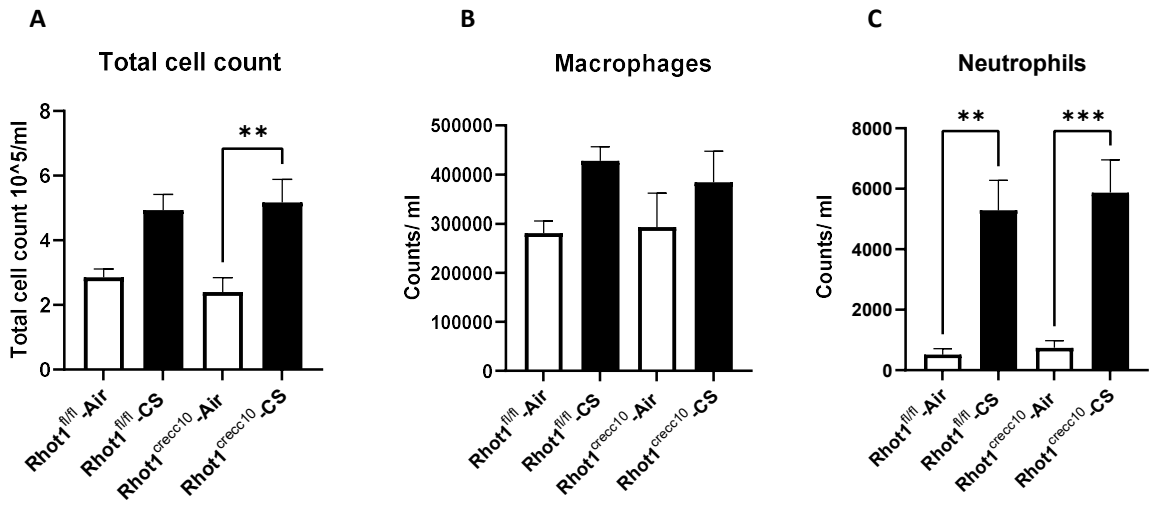

Figure 3: Increased neutrophil influx in Rhot1^{CreCC10} (Rhot1 Flox CreCC10$^{+/-}$) mice in response to CS exposure for 4 months

A: The number of total cells in BAL fluid from air and CS-exposed mice for 4 months was determined. **B:** Lavaged macrophage and **C**: neutrophil numbers were counted in Diff-Quik stained cytospin slides, which were prepared using BAL fluid. Quantification of macrophages neutrophils expressed as % of total cells in BAL fluid from air and CS exposed mice. CS exposed Rhot1^{CreCC10} (Rhot1 CreCC10$^{+/-}$) mice showed significant increase in total no of cells and number of neutrophils. Data are shown as mean ± SEM (n=3 to 5 per group).**$P < 0.01$, ***$P < 0.001$significant compared with corresponding air exposed mice

Figure 4

A

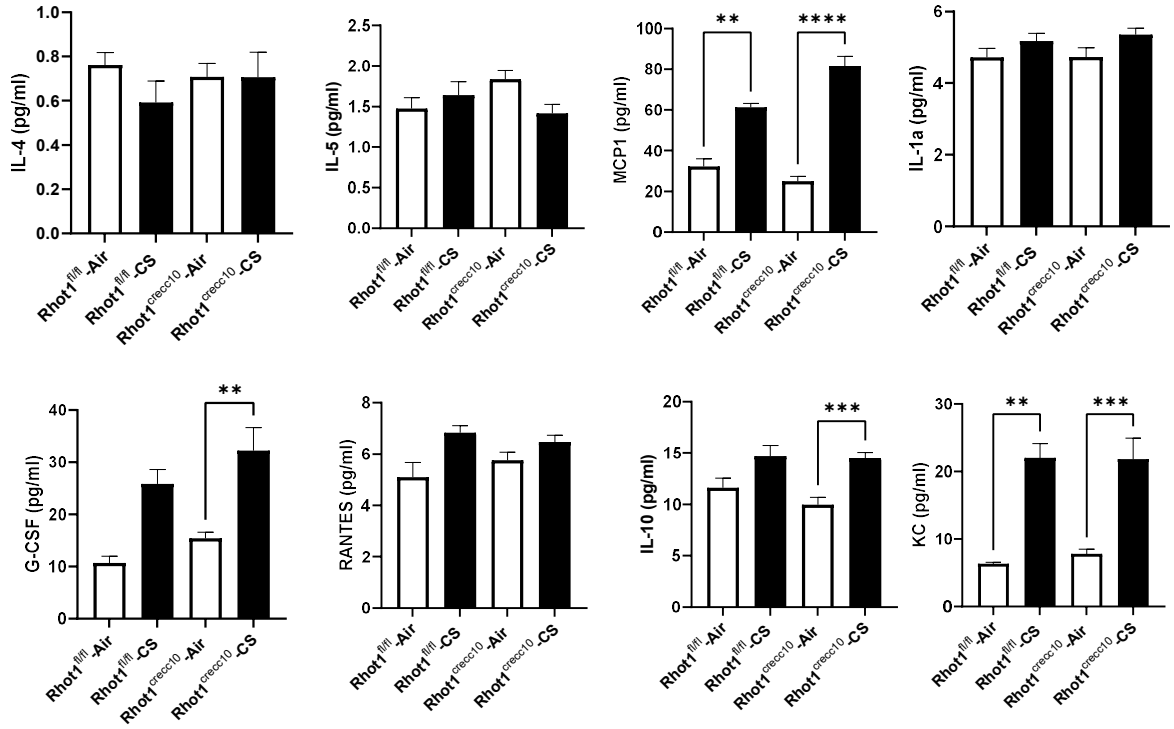
IL-4 (pg/ml)
IL-5 (pg/ml)
MCP1 (pg/ml)
IL-1a (pg/ml)
G-CSF (pg/ml)
RANTES (pg/ml)
IL-10 (pg/ml)
KC (pg/ml)
Rhot1fl/fl_Air
Rhot1fl/fl_CS
Rhot1crecc10_Air
Rhot1crecc10_CS
**
****
***

Figure 4

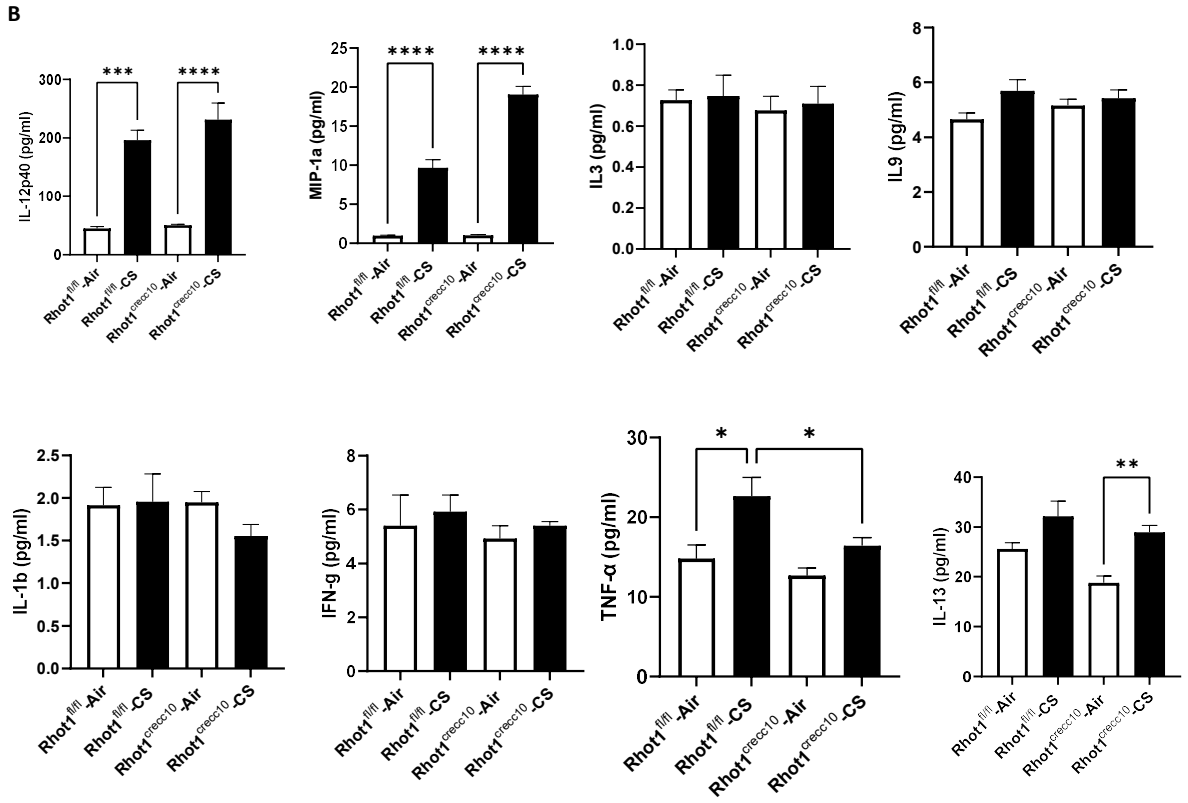

Figure 4

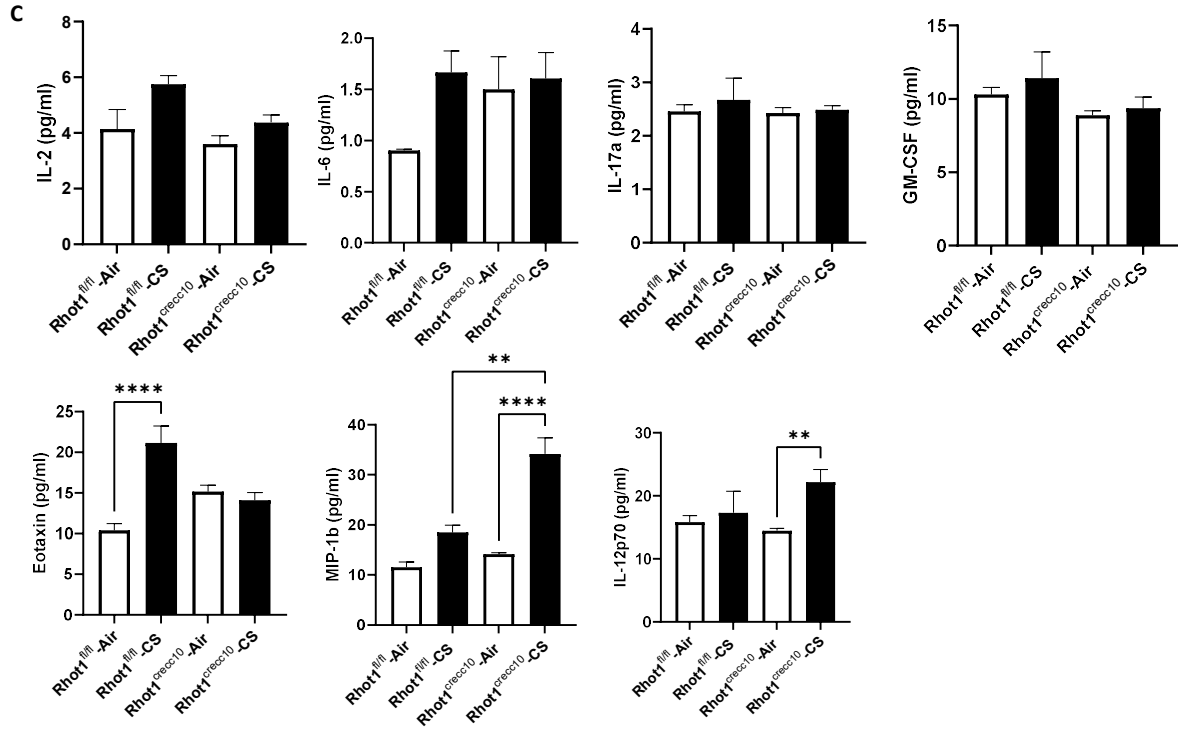

Figure 4A-C: Differential expression of cytokines in epithelial cell–specific Rhot1 deleted and WT mice: Rhot1$^{Fl/Fl}$ (WT) and Rhot1^{CreCC10} (Rhot1 flp CreCC10$^{+/-}$ and Rhot1 flp CreCC10$^{+/+}$) mice were exposed to room air and CS (mainstream) for 4 months (sub-chronic exposure). Expression levels of pro-inflammatory and inflammatory mediators in BAL fluid rom air and CS-exposed mice for 4 months as determined using Bio-Plex Pro 23-plex cytokine assay. Significance compared between corresponding Air and CS groups and all the groups compared with each other irrespective of their exposures. Data are shown as mean ± SEM (n=5 to 13 per group). *$P < 0.05$, **$P < 0.01$, ***$P < 0.001$, ****$P < 0.0001$.

Figure 5

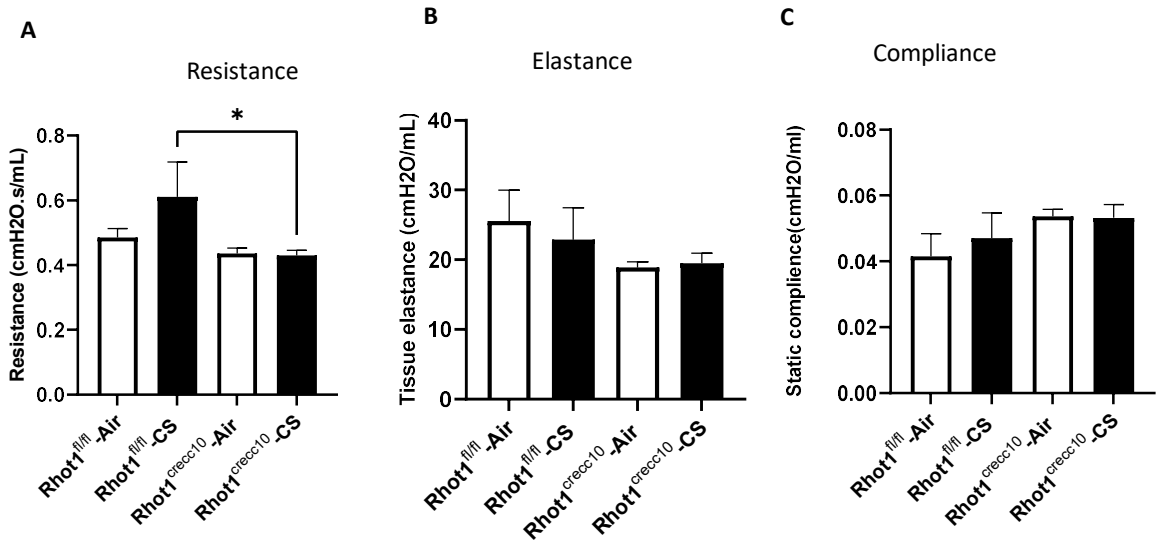

Figure 5: Alterations in lung mechanical properties in Rhot1^{CreCC10} (Rhot1 Flox CreCC10$^{+/}$) mice in response to CS exposure for 4 months

A: Tissue resistance **B:** elastance and **C**: static compliance were measured by FlexiVent after 4 months of air and CS exposure. Significance compared between corresponding Air and CS

groups and all the groups compared with each other irrespective of their exposures, $*P < 0.05$. Data are shown as mean ± SEM (n=3 to 7 per group). Changes between Air and CS groups were not found significant in any of the groups.

Figure 6

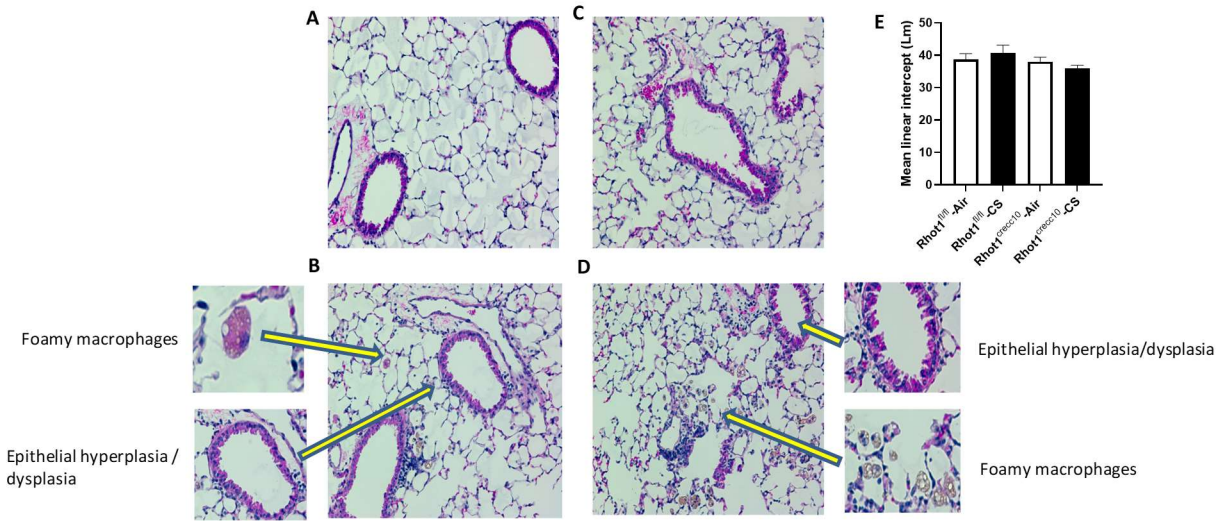

Figure 6: CS induced airspace enlargement and changes in histopathology in lungs of Rhot1^{CreCC10} (Rhot1 Flox CreCC10+/- and Rhot1 Flox CreCC10$^{+/-}$) mice exposed to CS for 4 months: Areas of interest are marked in red

The pictures shown are H&E stained lung sections from air and CS exposed Rhot1$^{Fl/Fl}$ (WT) and Rhot1^{CreCC10} (Rhot1 flox CreCC10+/- Rhot1 Flox CreCC10$^{+/-}$) mice for 4 months. **A.** Rhot1$^{Fl/Fl}$ -Air, **B**. Rhot1$^{Fl/Fl}$ -CS, **C**. Rhot1^{CreCC10} –Air, **D.** Rhot1^{CreCC10} –CS. Original magnification is 20X. **E**. Mean Linear Intercept (Lm) was analyzed in H&E stained. Lung sections from Air and CS-exposed Rhot1 Flox CreCC10$^{+/-}$ mice did not show significant airspace enlargement in comparison with air and CS-exposed Rhot1$^{Fl/Fl}$ (WT) mice. Data are shown as mean ± SEM (n=6 to 14 per group). However, other histopathological changes such as accumulation of pulmonary

macrophages and signs of epithelial hyperplasia dysplasia at airway regions of the CS exposed mouse lung were observed. The changes are more intensified in Rhot1 CC10+/- Flox Cre mice.

Figure 7

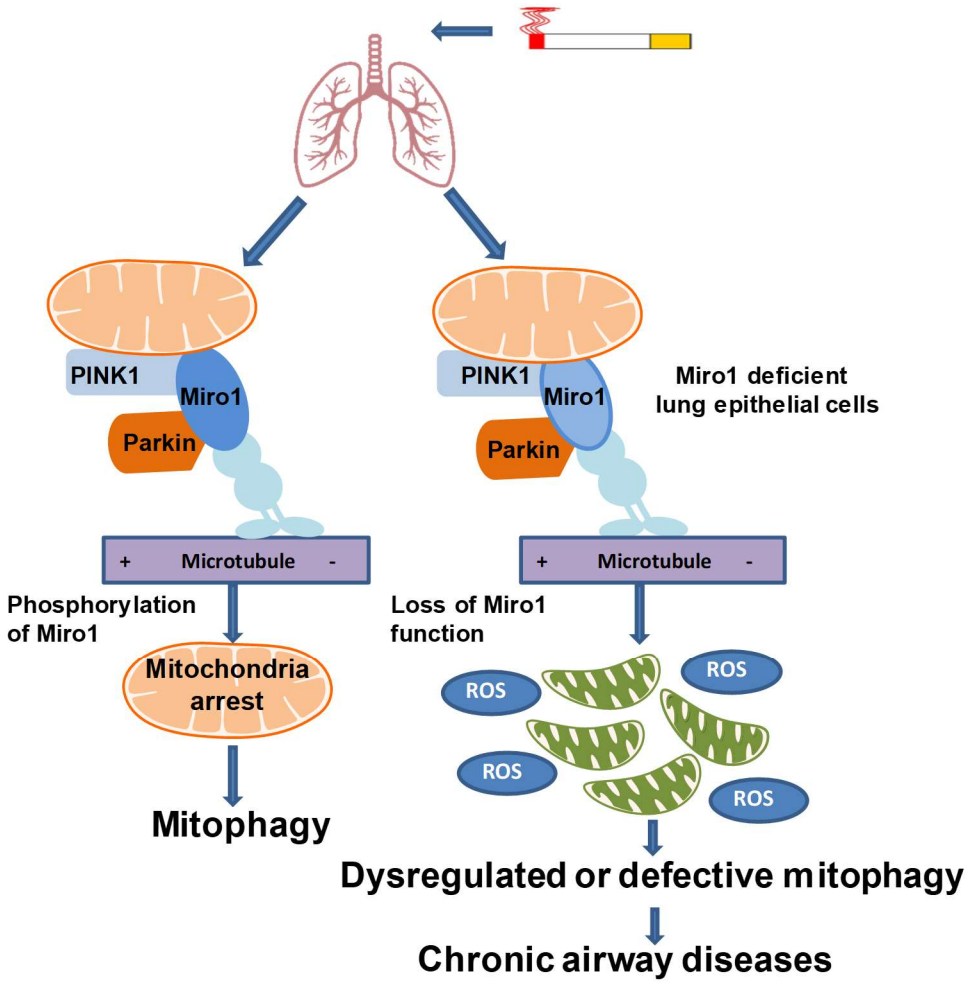

Figure 7: Cigarette Smoke induced Miro1 mediated mitochondrial dysfunction in lung epithelial cells**.**